



**A Fresh Look at
Angles-Only Orbit Determination**

**Chris Sabol, Scott Carter
Air Force Research Laboratory**

**David Vallado
US Space Command**

**AAS/AIAA Astrodynamics
Specialist Conference**

Girdwood, Alaska

16-19 August 1999

AAS Publications Office, P.O. Box 28130, San Diego, CA 92129

A FRESH LOOK AT ANGLES-ONLY ORBIT DETERMINATION

Dr. Chris Sabol[‡], Capt. Scott Carter^{*}, and Lt. Col. David Vallado ^{**}

Although the roots of angles-only orbit determination extend back to the times of Laplace in the late 1700's, most of today's astrodynamics community has been uncertain as to the applicability of angles-only estimation techniques for accurate satellite orbit determination. This approach provides a modestly robust method of sequentially processing angles-only information and, combined with increased availability of high accuracy angular observations in recent years, provides an attractive method for certain orbit determination applications. In addition, the combination of such accurate angular information with other sources (e.g. ranging data) offers the prospect of significant improvement in the ability to predict an object's motion. This paper addresses the use of angles-only information in the orbit determination processes by utilizing real world test cases from Air Force Research Laboratory (AFRL) assets. Specifically, single-site angles-only sequential estimation is performed to produce accurate orbit predictions of future passes over the site. The results demonstrate the utility of precise angles information in the context of high accuracy orbit determination.

INTRODUCTION

The concept of angles-only orbit determination has existed for several hundred years—ever since it was published by Pierre Simon de Laplace in 1780. Most of the early work in the angles-only area focused on producing initial orbital elements for minor planets and comets. Unfortunately, the solution isn't trivial, and although Laplace discovered it, it really couldn't be practically tested until the advent of the modern computer. Over the years, three main techniques were developed to process angles information for the purpose of initial orbit determination: Laplace's original method, Gauss' method, and double-iteration¹⁷.

Although these techniques are certainly remarkable achievements and highly effective for the applications of the time period when they were developed and for providing initial guesses for objects with little or no a priori knowledge, none yield sufficient accuracy for modern day orbit determination purposes. In order to achieve this level of accuracy, statistical techniques must be combined with larger quantities of data to estimate orbital parameters. The two most common methods used are weighted batch least squares (differential correction) and extended sequential processing (filtering).

[‡] Engineer, Air Force Research Laboratory / Directed Energy Directorate. Ph:(505) 846-4056, Fax: (505) 846-6053, sabolc@plk.af.mil

^{*} Engineer, Air Force Research Laboratory / Space Vehicles Directorate. Ph:(505) 853-3970, Fax: (505) 846-0033, carters@plk.af.mil

^{**} USSPACECOM/AN. Ph:(719) 554-3638, Fax: (719) 554-5068, david.vallado@spacecom.af.mil

Recent improvements in the availability of high accuracy optical sensors has brought new focus to the role of angular data in moderate to high accuracy orbit determination applications. Reference 1 discusses the development and use of the Raven optical sensor for deep space orbit determination. The Space-Based Visible (SBV) sensor on board the Midcourse Space Experiment (MSX) is another new high accuracy sensor collecting angles data². Magnetically controlled gimbal technology developed through the AFRL Small Business Innovative Research (SBIR) program provides new hardware capable of producing very accurate angular information³. Several sensors at the Maui Space Surveillance Site (MSSS) also have the capability to produce high accuracy angles data; the Hi-Class program, in particular, has demonstrated the ability to collect both accurate angular and ranging data to support space surveillance applications in the low earth orbit regime⁴.

In addition to new hardware developments, new studies have been undertaken to take advantage of these observation sources. Reference 5 takes an in-depth look at the use of accurate angles data in the geosynchronous orbit regime through simulated and real data analysis (subsets of that effort are contained in References 6 and 7). The primary focus of that work was the combination of range and angles data to produce high accuracy geosynchronous orbits although simulation studies did address the possibility of angles-only orbit determination. Reference 8 discusses orbit determination and prediction results of the Russian Space Surveillance System (RSSS) utilizing their semianalytic satellite theory and high accuracy angular observations from a wide network of optical sensors. The MSX SBV sensor's contributions to US Space Command's space surveillance operations are discussed in Reference 9, and Reference 10 contains analysis on angles-only orbit determination using the MSX SBV sensor.

This work extends the efforts of Wallace and Sabol to include orbit determination using real-world angles-only information from the Raven low cost optical sensor program. Unlike previous efforts, however, this work uses filtering techniques to process the high accuracy angular data. Starting with a moderate or low accuracy pointing vector, a satellite is acquired and tracked with an optical sensor (this is most easily achieved when the satellite is sunlit). The pointing vector is then used to initialize a filter run which updates the orbit based on the single-site, angles-only observations. The resulting orbit can then be used to provide more accurate predictions of the next satellite pass over the tracking station.

This idea is not unique in scope. Reference 11 demonstrates that precise orbits can be derived using single site high accuracy ranging combined with high fidelity filtering techniques. This study does not contain the same level of processing sophistication nor does it achieve the same level of accuracy as the above study but it does demonstrate that quality orbit predictions can be derived and maintained by a single optical site.

Using one tracking station can limit the regions of high accuracy to only over the tracking station; however, while not demonstrated here, the principles of the study can be applied to the multiple station tracking problem to provide accurate global predictions as well. This idea is consistent with ODIN, the distributed space surveillance architecture suggested by Reference 12. While by no means a proof of concept, this study does provide a cornerstone piece for such an architecture.

APPROACH

For orbit determination studies, it is always desirable to have a "truth" or reference orbit to which to compare results against. If the truth orbit is sufficiently accurate, conclusions can be made based upon the results of the comparisons. In this study, observation data sets were available on a variety of satellites with such truth orbits. GPS PRN 21 and TDRS-5 were chosen as test cases. In addition to serving as references for orbit comparisons, the truth orbits were used to calibrate the sensors. Once weights and biases were found for the angular observations, the angles data could then be processed through the filter program in an effort to produce accurate orbits.

Two strategies were used to initialize the filter process, both based on US Space Command space surveillance products. The first method considered the use of a standard Two-Line Element set (TLE) as the initial state. TLE's are easily accessible to authorized users with internet access but have typical errors on the kilometer level¹³. Since the estimation process used here employed a numerical integrator, the mean elements of the TLE's were converted to osculating via a Precise Conversion of Elements (PCE) run. The PCE consisted of an initial propagation of the TLE and then a differential correction to the resulting ephemeris using the numerical integrator. This produces the numerical integrator's best representation of the TLE. The second strategy involved initializing the filter runs with a Special Perturbations (SP) vector. SP vectors are the higher accuracy US Space Command product but are not routinely available on all satellites (at least not through the Air Force). In both cases, initial covariances were assumed since they are not provided with the space surveillance products.

Both the initial conditions (i.e. TLE's and SP vectors) and the results of the filter runs were propagated and compared to the truth orbits. The accuracy improvements in the updated orbits over those generated by propagating the initial conditions provides a measure of the value of the angular observations and the filtering technique.

The discussion above provides a general overview of the approach taken in this analysis. The next two subsections discuss the astrodynamics tools used in the analysis and details of the observation data sets. The last subsection outlines the estimation strategy used in the filtering process.

Tools

The Draper R&D version of the Goddard Trajectory Determination System (DGTDS) supports both differential correction and filtering techniques as well as a variety of propagation and observation models. The differential correction method consists of a weighted batch least squares that minimizes the residual differences between the computed and measured quantities over a period of time. The filter employed in DGTDS updates the estimated parameters based upon observations as they become available^{14,15}. These statistical techniques are combined with accurate force modeling and integration methods to provide orbit determination products with accuracy comparable to many commercially available software packages.

Table 1 summarizes the DGTDS configuration used in the filter and ephemeris generation runs for the GPS-21 and TDRS-5 satellites. The primary difference between the ephemeris generation portion of the run and the filter portion is the use of integrator. DGTDS does not currently support the Cowell integrator in the filter program. The only difference between the GPS and TDRSS runs is the maximum degree and order of the gravity model used.

DGTDS also contains versions of the NORAD general perturbations propagators used by US Space Command to produce space surveillance products such as TLE's^{13,16}. The combination of numerical integrators and the NORAD theories in one tool was especially valuable for comparison purposes and in performing mean to osculating element conversions required to initialize the numerical integrator based filtering process.

Data

Although several sources of data were available for this analysis, the primary consideration for selection was based upon the ability to accurately model the observations collected. As previously mentioned, multiple AFRL assets have the ability to provide angular measurements; however, when measurements from available sensors were compared to high fidelity orbit products, it was clear that there were systematic errors (likely due to mismodeling of the data). One observation source was available and well understood for use in this effort, however: the Raven telescope¹.

Table 1

DRAPER R&D GTDS CONFIGURATION SUMMARY

Satellite	GPS PRN 21	GPS PRN 21	TDRS 5	TDRS 5
Program	Filter	Ephemeris Generation	Filter	Ephemeris Generation
Integrator	Runge-Kutta 3(4+) Order	12th Order Summed Cowell/Adams Predict-Partial Correct	Runge-Kutta 3(4+) Order	12th Order Summed Cowell/Adams Predict-Partial Correct
Coordinate System	B1950.0	B1950.0	B1950.0	B1950.0
Step Size	10 sec	200 sec	10 sec	600 sec
Geopotential	12x12 JGM2	12x12 JGM2	8x8 JGM2	8x8 JGM2
Atmospheric Drag	None	None	None	None
Third-Body	Solar/Lunar point masses based on JPL DE ephemerides	Solar/Lunar point masses based on JPL DE ephemerides	Solar/Lunar point masses based on JPL DE ephemerides	Solar/Lunar point masses based on JPL DE ephemerides
Solar Radiation Pressure	Cylindrical shadow model, single Cr	Cylindrical shadow model, single Cr	Cylindrical shadow model, single Cr	Cylindrical shadow model, single Cr

The measurements used in this work consist of right ascension and declination observations of the GPS PRN 21 and TDRS-5 satellites during the 1996-1997 (TDRS-5) and 1998 (GPS 21) time frames. These objects were chosen primarily due to the availability of high accuracy reference orbits. Three consecutive nights of tracking were available for GPS 21 from January 13-15, 1998 from the Raven on Kirtland AFB, Albuquerque, NM. Consecutive nights of TDRS-5 tracking were not available but two sets of single night tracking (December 17, 1996, and March 7, 1997) were investigated. The data for TDRS-5 was taken from the Raven telescope in Kihei, Maui. All images were processed using the Raven astrometry code. Table 2 summarizes the measurements collected.

Table 2

RAVEN DATA SUMMARY

Satellite	GPS 21	TDRS-5	TDRS-5
Time Period	January 13-15, 1998	December 17, 1996	March 7, 1997
# Observations	104 (52 α + 52 δ)	228 (114 α + 114 δ)	80 (40 α + 40 δ)
# Passes	3	1	1

Prior to ingestion into DGTDS, these measurements were preprocessed from their original form into a coordinate system compatible with the version of DGTDS being used. The image processing software produced measurements in the mean equator, mean equinox of J2000 coordinate system. Because

the desktop PC version of DGTDS being used for this analysis does not currently support this coordinate system option, the observations were converted into the B1950 (mean equator, mean equinox of 1950) coordinate system. The transformation between these two systems can be found in Vallado¹⁷.

In addition to the angular measurements, truth data in the form of International GPS Service (IGS) precision ephemerides and NASA TDRS-5 osculating state vectors were collected for the periods of interest. The IGS produces orbit products accurate to 20 cm on the entire GPS constellation within 14 days and can be downloaded from the IGS web site^{18,19}. NASA Goddard Space Flight Center produces state vectors that are accurate to within 100 m on the TDRS spacecraft and are available from their on-line multimission flight dynamics product center²⁰. The IGS and NASA information was used for construction of reference orbits to calibrate and compare angles-only orbits against.

For GPS 21, the truth orbit was developed by performing a least squares fit to IGS precise orbit ephemerides. A fit to the data was performed to generate the best DGTDS representation of the IGS precise orbit and to facilitate comparison of the angles-only fits using a comparison program internal to DGTDS. The accuracy of the resulting product was evaluated by measuring the final residuals over the period of interest, and was seen to be on the submeter level. The TDRS-5 reference orbit was developed by propagating several state vectors provided by NASA personnel using DGTDS. The propagation was then validated by comparing the propagations of two independent state vectors over a common period of interest. The TDRS reference orbit is generally within 100 meters accuracy.

Finally, US Space Command Two Line Element sets (TLE's) were downloaded from Celestrak.com to use as initial conditions to the filter runs²¹. SP vectors were not available for either test cases and were simulated based on error analysis and past experience with those products.

Filter Configuration

As previously stated, an extended sequential filtering strategy was used to process the angles-only information given either a TLE or SP vector as an initial condition. With limited amounts of angles-only data available, it was decided to estimate only Keplerian orbital elements and not other factors such as solar radiation pressure reflectivity constants; over the short time spans of the satellite passes, the angles-only data did not allow for sufficient estimation of such parameters. In the cases studied here, reflectivity coefficients were estimated in the PCE process and used in the filter runs.

The covariance values for the initial conditions were assumed and coarsely refined to provide the best results. All off-axis values of the covariance matrix were assumed to be zero and Table 3 contains the standard deviations of the orbital elements used to complete the diagonal matrix.

Table 3

ASSUMED STANDARD DEVIATIONS OF THE INITIAL CONDITIONS

Orbital Element	GPS 21 TLE	GPS 21 SP	TDRS-5 TLE
Semimajor Axis	0.316 m	1 m	1 m
Eccentricity	1.0E-6	1.0E-6	3.16E-7
Inclination	3.16 millirad	1 microrad	1 millirad
Right Ascension of the Ascending Node	3.16 millirad	1 microrad	3.16 millirad
Argument of Perigee	3.16 millirad	0.1 millirad	3.16 millirad
Mean Anomaly	3.16 millirad	0.1 millirad	3.16 millirad

Weights and biases for the angles-only data were determined from calibration runs that compared the observations to the reference orbit. While the observation standard deviations were fairly small, which reflects their accuracy, the filter was instructed to accept all observations rather than edit any out due to a standard deviation edit criteria. This was required to allow the filter to accept the observations when the initial conditions were poor but still not provide too much freedom to the estimator resulting in divergence.

The extent of the force modeling used and integrator description is contained in Table 1 under the discussion of the DGTDS software system. For further details of the filter program inside DGTDS, refer to Reference¹⁵.

RESULTS

In this section, results are given from comparisons of the truth orbits to:

- the angles-only data for calibration purposes
- the orbits generated from the TLE and simulated SP vector initial conditions
- the orbits produced from the angles-only estimation process

for each of the three data cases (one GPS 21 and two TDRS-5). The calibration results show the quantity and the quality of the data used. Errors in the initial conditions provide a standard on which to improve upon, and the errors in the estimated products orbits demonstrate the merits of this approach.

GPS 21

Calibration of the Raven data for GPS PRN 21 revealed what appears to be a timing problem with the Raven sensor noted by Wallace et al. To counter this, as Reference 1 suggest, the single sensor is treated as two sensors to account for the different apparent biases in the Raven CCD shutter open and close times. This allows for easier calibration of the data and reveals the true noise levels of the sensor. Table 4 gives the standard deviations of the right ascension and declination observations. The results are consistent with previous estimates of Raven accuracy^{1,5,6}. Figure 1 plots the differences between the angular observations and the truth orbit after the biases have been removed.

Table 4

CALIBRATION RESULTS

Satellite	Date(s)	Sensor	Rt. Ascension Standard Deviation	Declination Standard Deviation
GPS 21	January 13-15, 1997	Albuquerque Raven	1.8"	1.5"
TDRS-5	December 17, 1996	Maui Raven	2.2"	1.9"
TDRS-5	March 7, 1997	Maui Raven	2.8"	2.0"

The next step in the analysis process was to compare the orbits generated from the initial conditions to the truth orbit. Using the SGP4 propagator internal to DGTDS, a US Space Command Two-Line element set was propagated and compared to the truth orbit over a 24 hour period after the first tracking pass. Figure 2 shows the maximum differences are 10.5 km with 2.5 – 3 km errors over the Raven tracking station in Albuquerque.

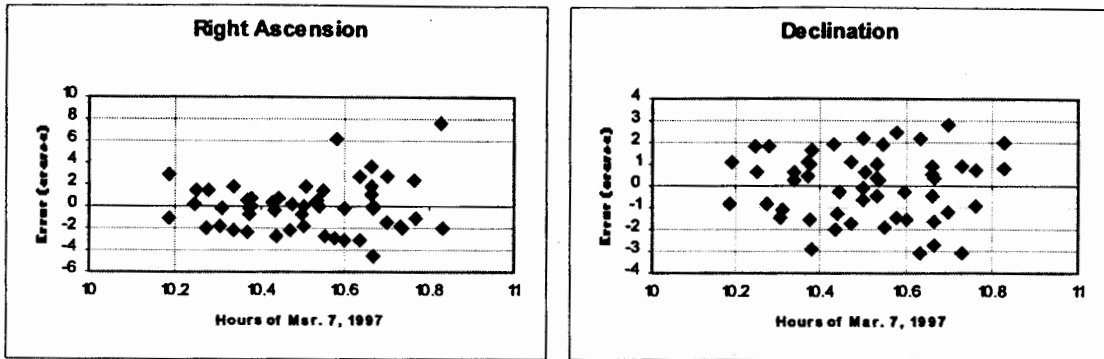


Figure 1 GPS 21 Angular Observation Errors

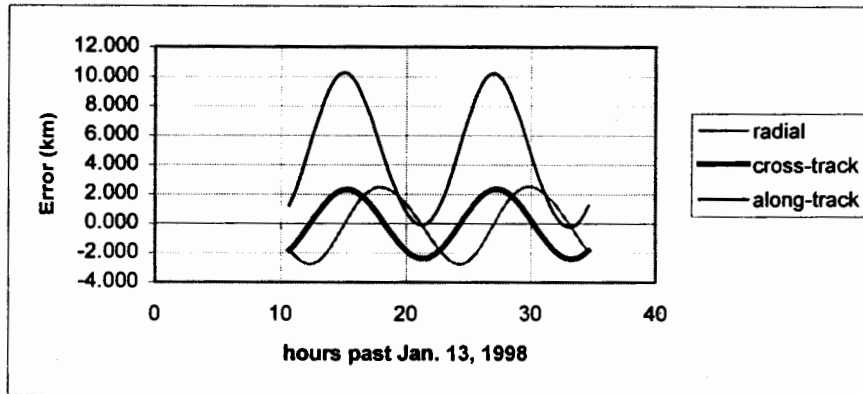


Figure 2 GPS 21 TLE Differences from Reference Orbit

Three filter runs were performed using the results of a mean to osculating Precise Conversion of Elements (PCE) of the TLE as initial conditions. The PCE was required to provide the best osculating representation of the TLE by the numerical integrator used in the filter runs. The three filter runs processed the first, first two and all three passes of angles-only data, respectively. At the end of each filter run, the resulting orbit was predicted ahead 24 hours to compare against the truth orbit. Table 5 has the resulting maximum global errors as well as the local or over-the-site error for the next satellite pass for all three filter runs and the TLE propagation. Figures 3-5 plot the orbit errors for the three filter runs. Figure 6 shows the position error for the TLE and the three filter runs at the end of the 24 hour prediction; this represented the predicted orbit error during the next pass over the tracking station.

Table 5

GPS 21 TLE AND TLE + ANGLES ERRORS

Case	Max. Global Error	Next Pass Error
TLE	10.5 km	2.5 - 3 km
TLE + 1 Pass	1.6 km	500 - 800 m
TLE + 2 Passes	1.0 km	125 - 210 m
TLE + 3 Passes	1.0 km	63 - 140 m

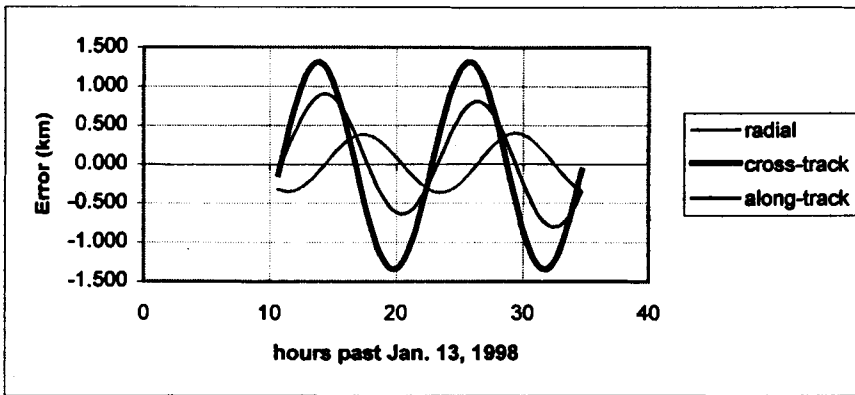


Figure 3 GPS 21 TLE + 1 Angles Pass Differences from Reference Orbit

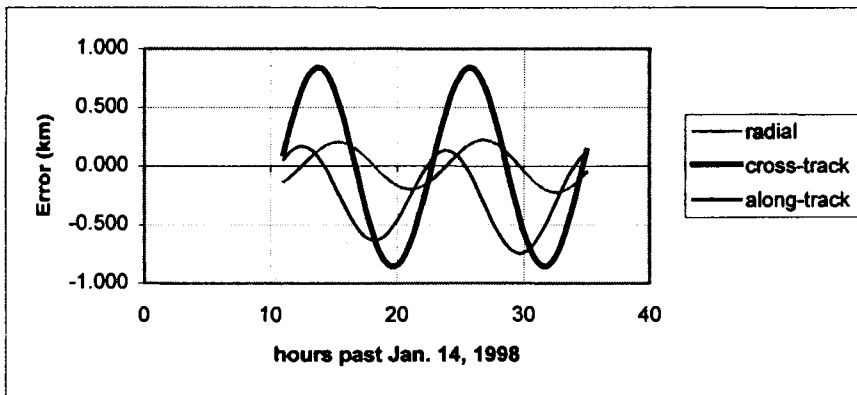


Figure 4 GPS 21 TLE + 2 Angles Passes Differences from Reference Orbit

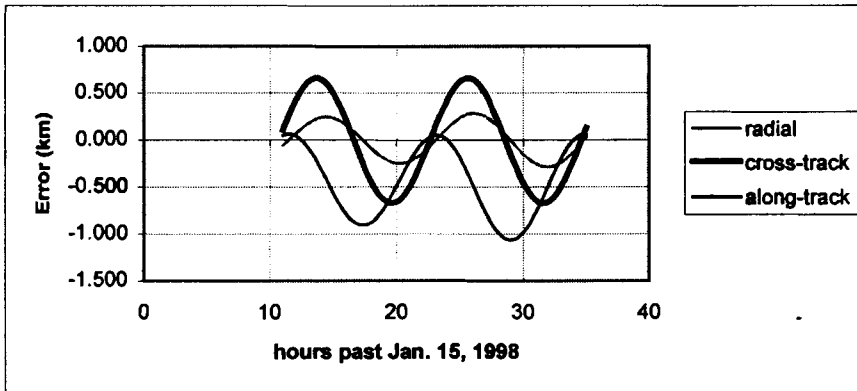


Figure 5 GPS 21 TLE + 3 Angles Passes Differences from Reference Orbit

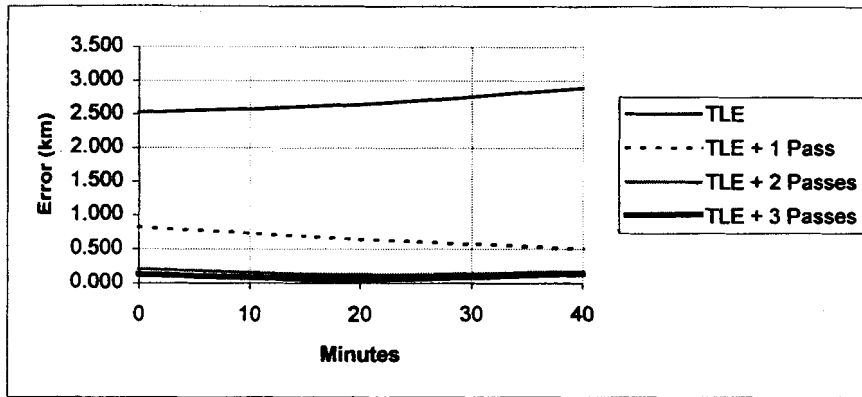


Figure 6 GPS 21 Differences from Reference Orbit During Following Pass

Figures 2-6 demonstrate that even with limited angles-only data, great improvements in orbit determination prediction accuracy can be made. Closer inspection of Figures 2 and 3 reveal that the a single pass of angles-only data has little impact on radial (and therefore along-track) prediction errors. However, Figures 4 and 5 show that multiple passes can help correct for radial errors.

The second part of the GPS 21 analysis considered using an SP vector to initialize the filter. Since an SP vector was not available, the reference orbit's initial conditions were perturbed to be representative of the expected errors of an actual SP vector. Figure 7 plots the differences between the simulated SP vector and the reference orbit. The appealing aspect of initializing the process with an SP vector is the fact that far less radial error is expected in the SP vector than what could be expected from a TLE.

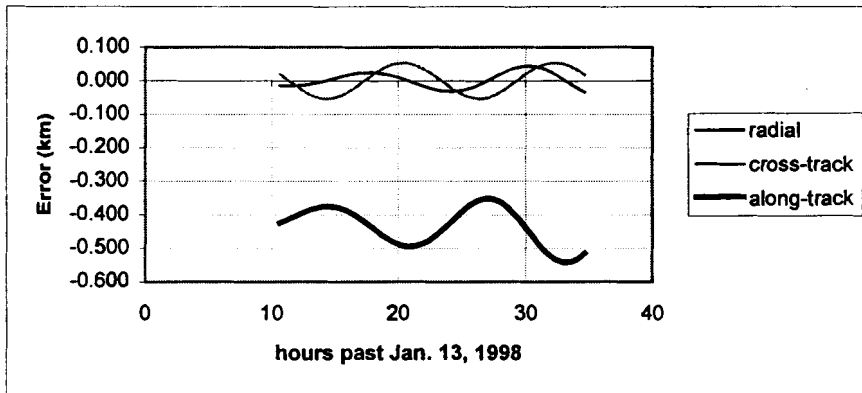


Figure 7 GPS 21 Simulated SP Vector Errors

Results from a one pass angles-only filter run using the simulated SP vector as the a priori value were impressive. Since the SP vector contained little radial error, the angles-only data corrected most of the initial orbital error and produced a very accurate orbit prediction. Table 6 contains the maximum global errors and the errors during the following pass over the tracking station for the simulated SP vector and the orbit produced after filtering through one pass of angles-only observations. Once again, the figures and the table show an order of magnitude improvement in the orbital products. In fact, after just one pass of angles data, the predicted orbit is likely accurate enough for easy acquisition from any site. Figure 8 plots the orbital errors after the simulated SP vector is updated from one pass of angle-only data and Figure 9 compares the prediction errors during the next pass over the tracking station.

Table 6

GPS 21 SP VECTOR AND SP VECTOR + ANGLES ERRORS

Case	Max. Global Error	Next Pass Error
SP	575 m	500+ m
SP + 1 Pass	70 m	< 50 m

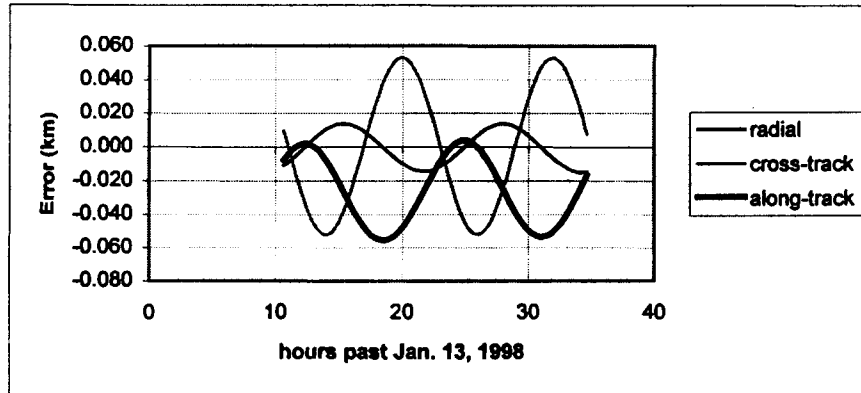


Figure 8 GPS 21 Simulated SP Vector + 1 Pass Angles Data Errors

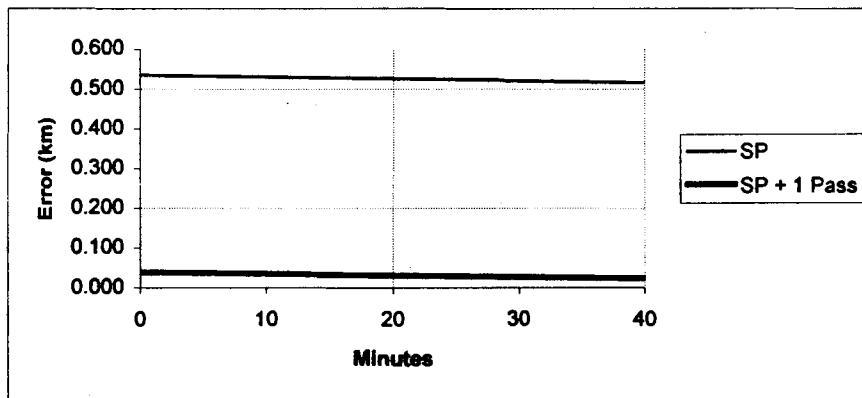


Figure 9 GPS 21 SP Vector and SP Vector + 1 Pass Angles Next Pass Prediction Errors

TDRS-5 12/17/96

Table 4 gives the standard deviations of the right ascension and declination observations of the TDRS-5 satellite. The results show the observations are good the two arcsecond level, which is not outstanding for the Raven telescope but can still be considered high accuracy for most optical sensors. Figure 10 plots the differences between the angular observations and the truth orbit after the biases have been removed.

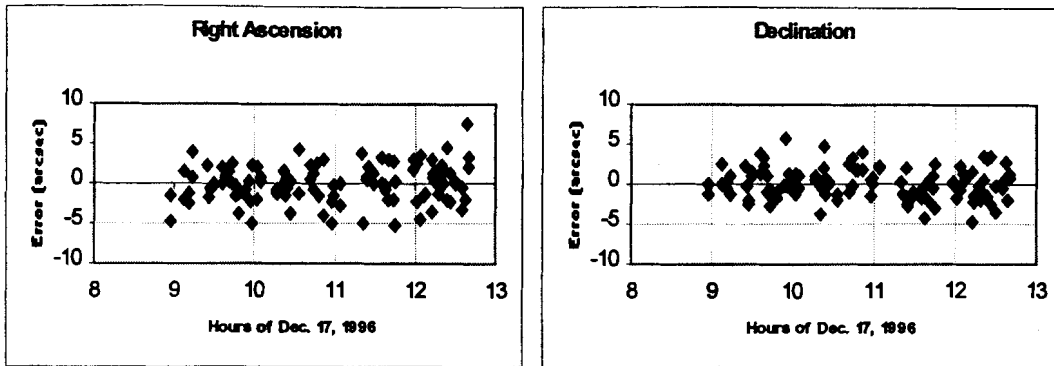


Figure 10 TDRS-5 Angular Observation Errors for 12/17/96

The next step in the analysis process was to compare the initial conditions to the truth orbit. Using the SGP4 propagator internal to DGTDS, a US Space Command Two-Line element set was propagated and compared to the truth orbit. Figure 11 shows the maximum differences are 59 km with 18 - 47 km errors over the pass span. These errors are slightly larger than what might be expected but that is due to the fact the TLE was close to two weeks old.

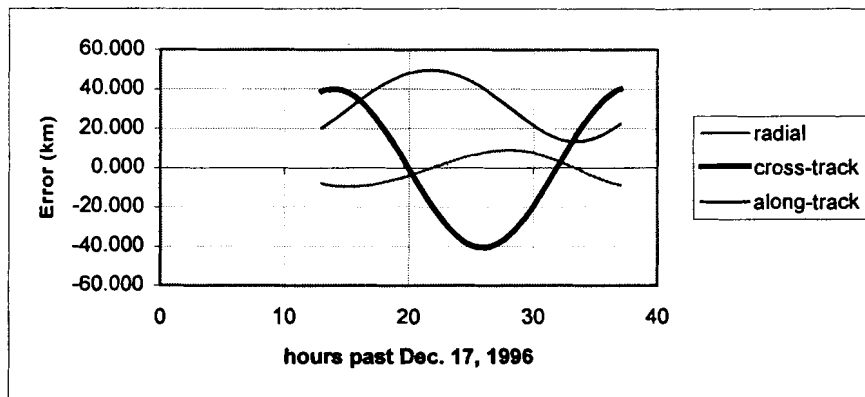


Figure 11 TDRS-5 TLE Differences from Reference Orbit for 12/17/96

Only one filter run is presented here since there was only one pass of angles-only data. The initial conditions were derived from the results of a mean to osculating Precise Conversion of Elements (PCE) of the TLE as which was required to provide the best osculating representation of the TLE by the numerical integrator used in the filter run. At the end of the filter run, the resulting orbit was predicted ahead 24 hours to compare against the truth orbit. Table 7 has the resulting maximum global error as well as the local or over-the-site error for the next satellite pass for the filter run and the TLE propagation. Figure 12 plots the orbit errors for the filter run and Figure 13 shows the position error for the TLE and the filter during the next pass over the tracking station.

Table 7

TDRS-5 TLE AND TLE + ANGLES ERRORS FOR 12/17/96

Case	Max. Global Error	Next Pass Error
TLE	59 km	18-47 km
TLE + 1 Pass	37.5 km	1.6-10 km

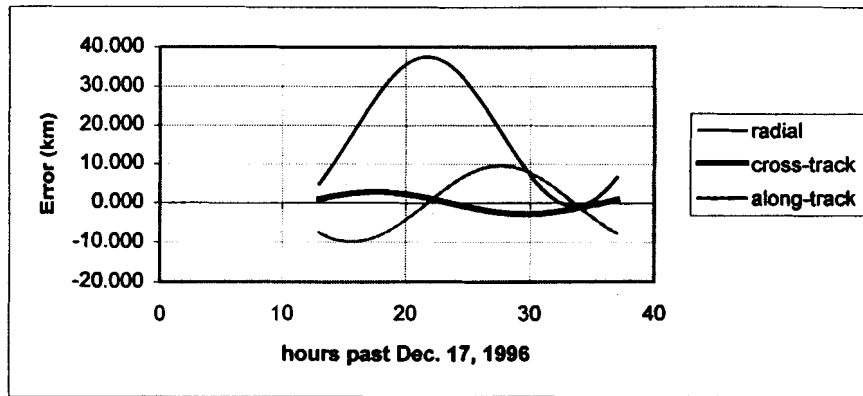


Figure 12 TDRS-5 TLE + 1 Angles Pass Differences from Reference Orbit for 12/17/96

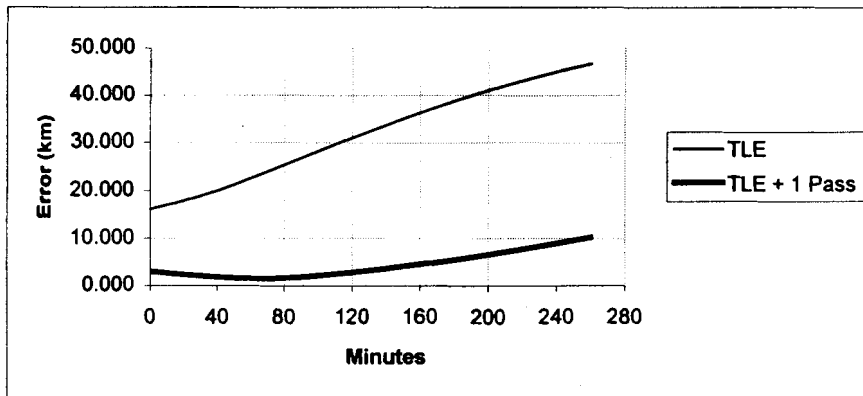


Figure 13 TDRS-5 Differences from Reference Orbit During Following Pass for 12/17/96

Once again the results demonstrate that even with limited angles-only data, great improvements in orbit determination prediction accuracy can be made; however, the limitations of the angles-only data to improve radial errors is even more apparent in the geosynchronous case. Note the large reduction in the magnitude of the cross-track errors; this is consistent with previous studies supplementing ranging data with high accuracy angular observations in a differential correction process⁶.

TDRS-5 3/7/97

Table 4 gives the standard deviations of the right ascension and declination observations of the TDRS-5 satellite. The results show the Raven noise levels with standard deviations around two arcseconds. Figure 14 plots the differences between the angular observations and the truth orbit after the biases have been removed.

The next step in the analysis process was to compare the initial conditions to the truth orbit. Using the SGP4 propagator internal to DGTDS, a US Space Command Two-Line element set was propagated and compared to the truth orbit. Figure 15 shows the maximum differences are 114 km with 90 km errors over the Albuquerque Raven tracking site. These errors are believed to be larger than a typical TLE for a geosynchronous satellite.

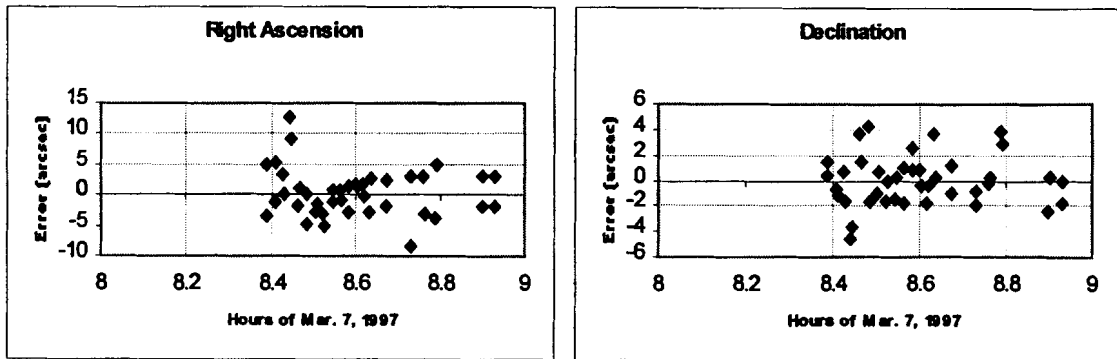


Figure 14 TDRS-5 Angular Observation Errors for 3/7/97

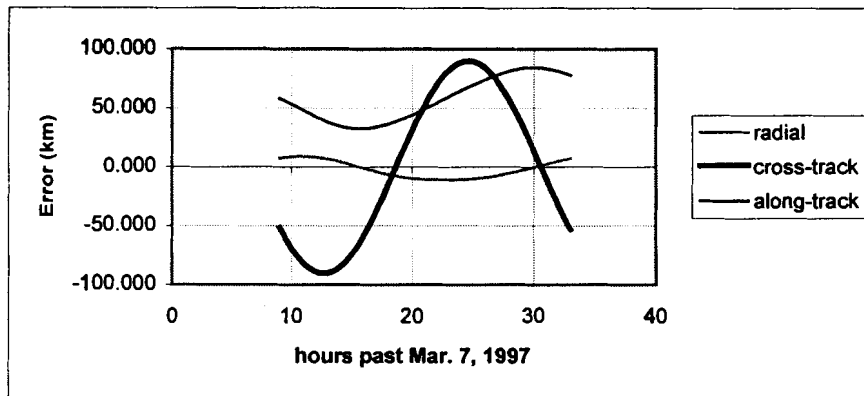


Figure 15 TDRS-5 TLE Differences from Reference Orbit for 3/7/97

Like the above TDRS results, only one pass of angles-only data was available during this time period which led to one filter run presented here. As before, the initial conditions were derived from the results of a mean to osculating Precise Conversion of Elements (PCE) of the TLE as which was required to provide the best osculating representation of the TLE by the numerical integrator used in the filter run. At the end of the filter run, the resulting orbit was predicted ahead 24 hours to compare against the truth orbit. Table 8 has the resulting maximum global error as well as the local or over-the-site error for the next satellite pass for the filter run and the TLE propagation. Figure 16 plots the orbit errors for the filter run and Figure 17 shows the position error for the TLE and the filter during the next pass over the tracking station.

Not surprisingly, the results are consistent with the previous cases. The angles-only data allows for an accurate update of the initials conditions and is limited by the radial error inherent in the a priori orbit or the amount of tracking data available to provide corrections. In this case, the radial errors are large which result in the dominant component of the prediction error being in the along-track direction. The initial error in the updated orbit is only 7 km but the along-track run-off increases that to 20 km by the following day. The primary benefit of the angles data in this case is the large reduction of the cross-track errors.

Table 8

TDRS-5 TLE AND TLE + ANGLES ERRORS FOR 3/7/97

Case	Max. Global Error	Next Pass Error
TLE	114 km	90 km
TLE + 1 Pass	26 km	20 km

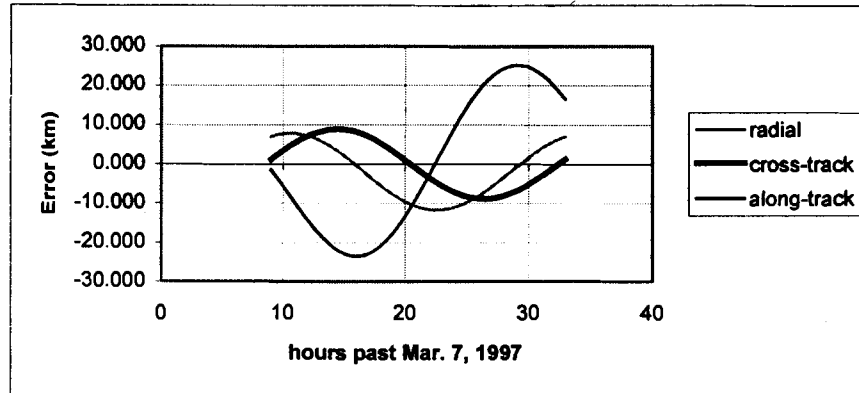


Figure 16 TDRS-5 TLE + 1 Angles Pass Differences from Reference Orbit for 3/7/97

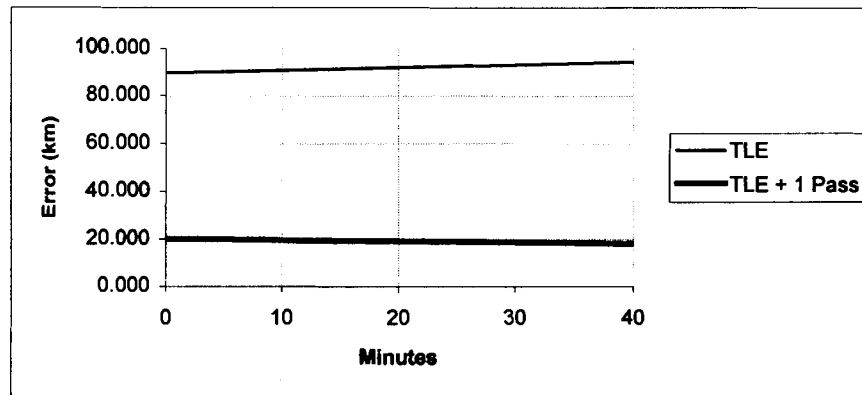


Figure 17 TDRS-5 Differences from Reference Orbit During Following Pass for 3/7/97

CONCLUSIONS

The results of this paper have shown that high accuracy angular observations can have great impact on the ability to determine and predict orbits. When applying sequential estimation techniques to one or more passes of high accuracy angles only data from a single tracking sensor, an order of magnitude accuracy improvement over the initial conditions used to initialize the filter was observed. These improvements were especially evident over the tracking station. A significant limitation of the angles-only approach is the inability to correct for radial errors in the initial conditions, but improvements can be made with successive tracking opportunities. Additionally, if the element set used to initialize the filter process is fairly accurate in a radial sense (like an SP vector) then the ability to produce and predict high accuracy orbits is greatly enhanced using this angles-only technique.

The ability to maintain a high accuracy orbit for acquisition purposes from a single site has been demonstrated using actual angles-only data and real US Space Command Two Line Element sets (TLE's). Although the test cases here dealt with deep space objects (a GPS satellite and a TDRS satellite), it is believed similar results can be demonstrated on low earth satellites given similar tracking conditions. Sensors exist which will allow for such an analysis but problems concerning the processing of those observations precluded their use in this study. This aspect of angles-only orbit determination is left to future work.

A further extension of this concept is ODIN, the distributed space surveillance architecture discussed by Alfano and Vallado. A cornerstone piece of the ODIN architecture is to have sensor sites download initial state vectors, acquire and track satellites, process the observations (most likely through sequential methods), and pass the improved orbit on to the next tracking station. This concept was essentially demonstrated here in a single site case. It is believed that multiple tracking stations would allow for even lower global errors in the orbit predictions. Of course, to fully implement a high accuracy space surveillance system, complimentary ranging and angular measurements are desirable. Even with the current NORAD space surveillance architecture, however, the results indicate that a single sensor (ideally a sensor capable of producing high accuracy range and angles like the Hi-Class program) can be used to vastly improve current space surveillance products upon request.

ACKNOWLEDGEMENTS

The authors would like to thank the Raven teams in Albuquerque and in Maui for all of their hours given to the hardware, software, and data collection and processing. Their dedication will provide for the growth of this technology. In addition to the Raven teams, the authors would like to thank the members of the other sensor teams for providing observation sets that unfortunately did not make their way into this work. Their cooperation and discussions could serve as models of professionalism in the research arena. The authors would also like to thank TS Kelso and his wonderful Celestrak web site and element set archival service for providing the TLE's used in this analysis.

REFERENCES

1. Wallace, S. T., C. Sabol, and S. Carter "Use of the Raven Optical Sensor For Deep Space Orbit Determination", AAS 97-705, AAS/AIAA Astrodynamics Specialist Conference, August 4-7, 1997, Sun Valley, ID.
2. Burnham, W. F., R. Sridharan, "Geosynchronous Surveillance with a Spaced-Based Sensor", AAS/AIAA Space Flight Mechanics Meeting, Austin TX, February 12-15, 1996. AAS 96-214.
3. Lawrence, John (Jack), personal discussion, March, 1998. Mr. Lawrence works for TRW, One Space Park, Redondo Beach, CA. E-mail: John.Lawrence@trw.com
4. Werling, D., et al, "Active Lasing of Space Objects Using the HI-CLASS (High Performance CO2 LADAR Surveillance Sensor) Laser System", Proceedings of the 1999 Space Control Conference, MIT Lincoln Laboratory, Lexington, MA, 13-15 April, 1999.
5. Sabol, C. A. *A Role For Improved Angular Observations in Geosynchronous Orbit Determination*, Doctoral Thesis, Department of Aerospace Engineering Sciences, University of Colorado, 1998.
6. Sabol, Chris, R. Burns, S. Wallace, "Analysis of the Telstar-401/GOES-10 Close Approach Using the Raven Telescope", AAS/AIAA Space Flight Mechanics Meeting, Monterey, CA, February 9-11, 1998. AAS 98-118.
7. Sabol, C., R. Culp, "Improved Angular Observations in Geosynchronous Orbit Determination", AIAA/AAS Astrodynamics Specialist Conference, Boston, MA, August 10-12, 1998. AIAA 98-4281.

8. Rundenko, Sergei P., et al "Some Results of the Analysis of the Geosynchronous Satellite Observations", Conference on Astrometry and Celestial Mechanics, Poznan, Poland, September 13-17, 1993. Proceedings published as *Dynamics and Astrometry of Natural and Artificial Celestial Bodies* by the Astronomical Observatory of the A. Mickiewicz University, Poznan, Poland, 1994.
9. von Braun, C., "Space Surveillance Operations with the Space-Based Visible", Proceedings of the 1999 Space Control Conference, MIT Lincoln Laboratory, Lexington, MA, 13-15 April, 1999.
10. Abbot, R.I., J Sharma, "Determination of Accurate Orbits for Close Encounters between Geosynchronous Satellites", Proceedings of the 1999 Space Control Conference, MIT Lincoln Laboratory, Lexington, MA, 13-15 April, 1999.
11. Hujsak, R.S., G.C. Gilbreath, "Sequential orbit determination for GPS-35 and GPS-36 using SLR data from NRL@SOR", SPIE Proceedings, 3380 (32), April 1998.
12. Vallado, D., S. Alfano, "A Future Look at Space Surveillance and Operations", AAS/AIAA Space Flight Mechanics Meeting, Breckenridge, CO, February 7-10, 1999. AAS 99-113.
13. Barker, William N., Stephen J. Casali, Richard N. Wallner, "The Accuracy of General Perturbations and Semianalytic Satellite Ephemeris Theories", AAS/AIAA Astrodynamics Specialist Conference, Halifax, Nova Scotia, Canada, August 14-17, 1995. AAS 95-432.
14. Computer Sciences Corp. and NASA Goddard Space Flight Center (Editors), *GTDS Mathematical Theory Revision 1*, Contract NAS 5-31500, Task 213, July 1989.
15. Dunham, J.B., *The Research and Development Goddard Trajectory Determination System (R&D GTDS) Filter Program Software Specifications and User's Guide*, prepared for Goddard Space Flight Center by Computer Sciences Corporation under Contract NAS 5-24300 Task Assignment 977. 1980.
16. Herriges, Darrell Lee, *NORAD General Perturbation Theories: An Independent Analysis*, M. S. Thesis, Dept. of Aeronautics and Astronautics, MIT, January, 1988.
17. Vallado, David A., *Fundamentals of Astrodynamics and Applications*, published by McGraw Hill, New York, 1997.
18. International GPS Service Data Products, available on the world wide web:
<http://igs.cb.jpl.nasa.gov/components/prods.html>
19. International GPS Service Products Available for Download, available on the world wide web:
http://igs.cb.jpl.nasa.gov/components/prods_cb.html
20. NASA Goddard Space Flight Center MultiMission Flight Dynamics Product Center:
http://mmfd.gsfc.nasa.gov/FDD_products.html
21. Celestrak Web Page: <http://www.celestrak.com>